Phonon dilatation, dressed vibrons, and two-vibron bound-state localization in an adsorbed nanowire

V. Pouthier*
Laboratoire de Physique Moléculaire, UMR CNRS 6624, Faculté des Sciences—La Bouloie, Université de Franche-Comté, 25030 Besançon cedex, France
(Received 5 May 2006; published 18 September 2006)

A special attention is paid to characterize the two-vibron bound-state dynamics of an anharmonic molecular nanostructure coupled with a set of optical phonons. It is shown that the vibron-phonon coupling is responsible for a new dressing mechanism. The vibrons are accompanied by virtual phonons which account for the scaling of each phonon coordinate and for the dilatation of the corresponding wave function. As a result, the dynamics of the dressed vibrons is governed by an effective Hamiltonian whose frequency, anharmonicity, and hopping constant depend on the number of optical phonons. The two-vibron bound states are defined according to a mean field procedure in which the number of phonons is fixed to their thermal average value. However, the thermal fluctuations of the number of phonons yield a vibron Hamiltonian equivalent to the Hamiltonian of a disordered lattice and they favor the localization of the bound states. For a weak vibron-phonon coupling, the localization results from quantum interferences and it follows a universal behavior. By contrast, for a strong coupling, the localization originates in the occurrence of infinite potential barriers which confine the bound states onto clusters whose number and size are controlled by the temperature.

DOI: 10.1103/PhysRevB.74.125418 PACS number(s): 73.21.Hb, 71.35.−y, 63.20.Ry, 63.22.+m

I. INTRODUCTION

In a series of recent papers,[1–7] it has been suggested that the nonlinear dynamics of high-frequency vibrational excitons (vibrons) could play a key role for the information transfer in adsorbed molecular nanostructures. This feature was first pointed out by Davydov[8] to explain the energy flows in proteins. The vibron dynamics was described by a discrete nonlinear Schrödinger equation (NLS), whose continuum limit leads to the so-called Davydov's soliton. In addition, the discrete NLS equation supports discrete breathers which correspond to time-periodic and spatially localized solutions resulting from the interplay between the discreteness and the nonlinearity. Since discrete breathers yield a local accumulation of the vibrational energy which might be pinned in the lattice or may travel through it, they are expected to be of fundamental importance.[9–11] However, in spite of the great interests that solitons and breathers have attracted, no clear evidence has yet been found for their existence in real molecular lattices.

By contrast, two-vibron bound states (TVBS) have been observed in several molecular monolayers adsorbed on the surface of a solid substrate. As examples, bound states in the systems H/Si(111),[12,13] H/C(111),[14] CO/NaCl(100),[15] and CO/Ru(001) (Refs. 16–20) have been characterized by using optical probes whereas bound states in the system H/Ni(111) were investigated by using high resolution electron energy loss spectroscopy.[21] In quantum lattices, the nonlinearity yields the interaction between the vibrons and favors the formation of bound states. When two vibrons are excited, a bound state corresponds to the trapping of two quanta over only a few neighboring molecules with a resulting energy which is lesser than the energy of two quanta lying far apart. The lateral interaction yields a motion of such a state from one molecule to another, thus leading to the occurrence of a delocalized wave packet with a well-defined momentum. TVBS are the first quantum states which experience the nonlinearity and they can be viewed as the quantum counterpart of breathers or soliton excitations.[3–6,22–27]

In a general way, two main nonlinear sources contribute significantly to the occurrence of bound states. The first contribution originates in the intramolecular anharmonicity of each molecule. As shown by Kimball *et al.*,[24] this effect can be accounted within the standard perturbative theory. The intramolecular potential is expanded up to the fourth order with respect to the internal coordinate and a unitary transformation is performed to keep the vibron-conserving terms, only. The resulting Hamiltonian is a Bose version of the Hubbard model with attractive interactions.[2–6]

The second contribution results from the coupling between the vibrons and the low-frequency external modes of the system. Usually, this effect is described by a Fröhlich type Hamiltonian[28] in which the vibrons interact with a phonon bath responsible for a modulation of the vibrational frequency of each molecule. These phonons are supposed to be harmonic and the vibron-phonon coupling Hamiltonian exhibits a linear dependence with respect to the phonon coordinates. To partially removed the vibron-phonon coupling, a unitary transformation is performed to reach a new point of view in which the elementary excitations are dressed vibrons called small polarons.[29–37] The formation of a small polaron proceeds as follows. Because the vibron bandwidth is usually smaller than the phonon cutoff frequency, the phonons propagate faster than the vibrons so that the nonadiabatic limit is reached. Therefore, during its propagation, a vibron leads to a lattice distortion, essentially located on a single site, which follows instantaneously the vibron. This distortion originates in the modification of the phonon state due to the vibron-phonon coupling and it corresponds basically to a local coherent state for the phonons. In such a coherent state, the number of phonons is not conserved so that, from a quantum point of view, the lattice distortion can be viewed as a

virtual cloud of phonons. The vibron dressed by the virtual cloud of phonons forms the small polaron.

In the present work, a new dressing mechanism is introduced to describe the TVBS dynamics in a molecular lattice adsorbed on a surface. To simplify our discussion, we consider a one-dimensional adsorbed lattice, i.e., a nanowire. Indeed, it has been shown by Persson and co-workers[38–45] that the high-frequency stretching mode of each admolecule is preferentially coupled with a low-frequency local mode. Such a mode, which can be viewed as an optical phonon, refers either to the frustrated translational motion of the center of mass of the admolecule or to its frustrated rotational motion. In that context, since the admolecules are adsorbed onto high symmetry adsorption sites, the vibron-phonon coupling depends in a quadratic way on the phonon coordinates. As a result, the creation of vibrons is accompanied by a modification of the phonon states responsible for a new kind of dressing.

The paper is organized as follows. In Sec. II, the Hamiltonian to describe the vibron-phonon dynamics in an adsorbed nanowire is introduced. In Sec. III, we first realize a unitary transformation within the zero vibron hopping constant limit to remove the vibron-phonon interaction and to reach a dressed vibron point of view. Then, this transformation is applied to the full Hamiltonian and a mean field procedure is used to define an effective Hamiltonian for the dressed vibrons. Finally, a random lattice model is established to characterize the coupling between these dressed vibrons and the remaining phonons. In Sec. IV, a numerical analysis of this model is presented where a special attention is paid to characterize the TVBS dynamics. The results are discussed and interpreted in Sec. V.

II. THE VIBRON-PHONON HAMILTONIAN

Let us consider a one-dimensional nanostructure formed by N molecules adsorbed on a well-organized substrate. Each molecule n behaves as a high-frequency anharmonic oscillator described by the internal coordinate q_n and by the standard vibron operators $b_n^\dagger$ and b_n. Within the model introduced by Kimball *et al.*,[24] the vibron Hamiltonian H_v is written as (using the convention $\hbar=1$),

$$H_v = \sum_n \omega_0 b_n^\dagger b_n - A b_n^\dagger b_n^\dagger b_n b_n + \Phi[b_n^\dagger b_{n+1} + \text{H.c.}], \quad (1)$$

where H.c. denotes the Hermitian conjugate, ω_0 is the internal frequency, A is the intramolecular anharmonicity, and Φ is the hopping constant between nearest neighbor molecules.

The vibron Hamiltonian H_v conserves the vibron population so that the Hilbert space E_v can be written as the tensor product $E_{v,0}\otimes E_{v,1}\otimes E_{v,2}\otimes\cdots\otimes E_{v,m}\ldots$, where $E_{v,m}$ denotes the subspace connected to the presence of m vibrational quanta. In this paper, we focus our attention on the two quanta states belonging to the subspace $E_{v,2}$ whose dimension $N(N+1)/2$ represents the number of ways for distributing two indistinguishable quanta onto N sites. The diagonalization of H_v shows that the lattice supports both two-vibron free states (TVFS) and TVBS (see, for instance, Refs. 2–6, 24, and 26). TVFS describe two independent vibrons delocalized over the lattice and the energy of which belongs to an energy continuum. By contrast, in a TVBS, the two quanta are trapped close to each other so that a localization of the separating distance between the two vibrons takes place. However, the lateral interaction yields a motion of the center of mass which is delocalized over the lattice.

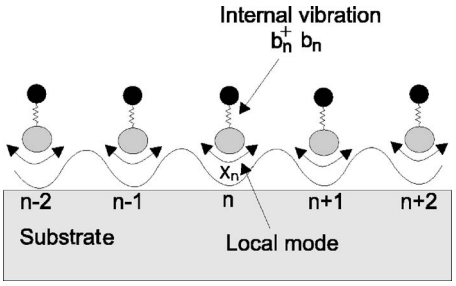

FIG. 1. Illustration of the geometry of a molecular nanowire adsorbed on the surface of a solid substrate. The sine curve mimics the potential experienced by the adsorbed molecules and it defines the adsorption sites. The figure shows the two kinds of motion considered in this work. First, the internal motion of each molecule corresponds to a high-frequency anharmonic oscillator characterized by the creation and annihilation operator $b_n^\dagger$ and b_n. Then, each internal mode is coupled with a low-frequency phonon whose local coordinate X_n refers either to the frustrated translation or to the frustrated rotation of each molecule trapped in its adsorption site.

By following Persson and co-workers,[38–45] we assume that the internal vibration of the nth molecule interacts with a low-frequency local mode. This mode corresponds to an optical phonon with mass M, frequency Ω_0, coordinate X_n, and momentum P_n (see Fig. 1). Within the harmonic approximation, the set of optical phonons is characterized by the Hamiltonian H_p written as

$$H_p = \sum_n \Omega_0 \left(\frac{p_n^2}{2} + \frac{x_n^2}{2} \right), \quad (2)$$

where $x_n=\sqrt{M\Omega_0/\hbar}X_n$ and $p_n=1/\sqrt{M\Omega_0\hbar}P_n$ denote the reduced coordinate and momentum, respectively. Note that H_p can be expressed in terms of the standard phonon operators $a_n^\dagger=(x_n-ip_n)/\sqrt{2}$ and $a_n=(x_n+ip_n)/\sqrt{2}$ as $H_p=\Sigma_n\Omega_0(a_n^\dagger a_n+\frac{1}{2})$. The Hamiltonian H_p describes N independent oscillators whose Hilbert space E_p can be written as the tensor product of the Hilbert space of each local mode. The eigenstates of H_p are thus expressed as $|p_1,p_2,\ldots,p_N\rangle$, where p_n denotes the number of low-frequency optical phonons onto the nth local mode.

According to Persson and co-workers, the frequency of the nth stretching mode depends on the local mode coordinate x_n. By assuming that the molecule is adsorbed onto a high symmetry adsorption site, such a dependence is invariant under the transformation $x_n\rightarrow -x_n$ so that the modulation is proportional to x_n^2 at the lowest order. The coupling Hamiltonian between the vibrons and the optical phonons is thus expressed as

$$\Delta H = \sum_n \frac{1}{2}\Delta x_n^2 b_n^\dagger b_n, \quad (3)$$

where Δ denotes the vibron-phonon coupling parameter.

For small adsorbed molecules, the anharmonic parameter, usually close to the gas phase value, ranges between 10 and 40 cm^{-1}, whereas the vibron bandwidth is typically lesser than or about 10 cm^{-1}. For instance, for the CO/Ru system (see Ref. 5, and references therein), the anharmonicity is $A=15.56$ cm^{-1} and the hopping constant is $\Phi=3.82$ cm^{-1}. For the H/Si(111) system, the vibron bandwidth is equal to 10 cm^{-1} and the anharmonicity was found to be $A=34$ cm^{-1}.[12,13] The characteristics of the low-frequency local mode depend on both the adsorbed molecule and the substrate. For CO/Ni,[38–40] the phonon corresponds to a frustrated rotation of the admolecule with a frequency $\Omega_0=235$ cm^{-1}. The strength of the vibron-phonon coupling is about $\Delta=40$ cm^{-1}. By contrast, for CO/Ru,[40–44] the local mode refers to the frustrated translation of the admolecule parallel to the surface. The corresponding frequency is $\Omega_0=47$ cm^{-1} and the vibron-phonon coupling is $\Delta=-6$ cm^{-1}. For H/Si,[45] the frequency of the optical phonon is $\Omega_0=210$ cm^{-1} and the vibron-phonon coupling is $\Delta=-10$ cm^{-1}. Note that in all these situations, each low-frequency local mode strongly interacts with the phonons of the substrate which results in a short lifetime of about a few picoseconds.

Finally, the full Hamiltonian $H=H_v+H_p+\Delta H$ yields a rather simple model for the vibron-phonon dynamics in an adsorbed nanowire. Nevertheless, it cannot be solved exactly due to the anharmonic vibron-phonon coupling ΔH and the following section is devoted to its simplification.

III. THEORETICAL BACKGROUND

A. The zero hopping constant limit: phonon dilatation and dressed vibrons

To understand the influence of the vibron-phonon coupling, let us first neglect the vibron hopping constant Φ in Eq. (1). As a result, the system reduces to a set of N independent sites and the Hamiltonian describing the nth site is written as

$$H_n = \omega_0 b_n^\dagger b_n - A b_n^{\dagger 2} b_n^2 + \Omega_0 \left(\frac{p_n^2}{2} + \frac{x_n^2}{2} \right) + \frac{\Delta}{2} x_n^2 b_n^\dagger b_n. \quad (4)$$

A natural basis to describe the nth site is formed by the eigenstates of H_n when $\Delta=0$. A particular eigenstate, denoted $|v_n,p_n\rangle$, refers to the presence of v_n high-frequency vibrons and p_n optical phonons. Therefore, Eq. (4) shows that the vibron-phonon coupling conserves the vibron number. By contrast, it induces the creation and the destruction of optical phonons and yields fluctuations of the phonon number. Such transitions originate in the modification of the potential energy of the nth local mode, i.e., $\Omega_0 x_n^2 \rightarrow (\Omega_0+\Delta v_n)x_n^2$, when a nonvanishing vibron population is created onto the nth site.

To account for this modification, let us introduce the following unitary transformation:

$$U_n = e^{-\theta(N_n)[1/2+ix_n p_n]}, \quad (5)$$

where $\theta(N_n)$ is an operator which depends on the vibron population $N_n=b_n^\dagger b_n$, only. The transformation U_n, known as the dilatation operator, yields a scaling of both the local mode coordinate and momentum as

$$U_n x_n^m U_n^\dagger = e^{-m\theta(N_n)} x_n^m,$$

$$U_n p_n^m U_n^\dagger = e^{m\theta(N_n)} p_n^m. \quad (6)$$

At this step, $\theta(N_n)$ remains an unknown operator which is determined in order to remove the vibron-phonon coupling term occurring in Eq. (4). By transforming the Hamiltonian H_n it is straightforward to show that the required operator is defined as

$$\theta(N_n) = \frac{1}{4} \ln\left[1 + \frac{\Delta}{\Omega_0} N_n \right]. \quad (7)$$

The transformed local Hamiltonian $\hat{H}_n=U_n H_n U_n^\dagger$ is finally written as

$$\hat{H}_n = \omega_0 b_n^\dagger b_n - A b_n^{\dagger 2} b_n^2 + \Omega(N_n)\left(\frac{p_n^2}{2} + \frac{x_n^2}{2} \right), \quad (8)$$

where $\Omega(N_n)=\Omega_0\sqrt{1+(\Delta/\Omega_0)N_n}$.

The transformation Eq. (5) yields an exact diagonalization of the local Hamiltonian within the unperturbed basis $|v_n,p_n\rangle$. The eigenstates of the nth site are thus defined as $|\Psi(v_n,p_n)\rangle=U_n^\dagger|v_n,p_n\rangle$ so that the corresponding wave functions are written as

$$\Psi_{v_n,p_n}(q_n,x_n) = \chi_{v_n}(q_n) \times \left[1 + v_n \frac{\Delta}{\Omega_0} \right]^{1/8} \varphi_{p_n}\left(\left[1 + v_n \frac{\Delta}{\Omega_0} \right]^{1/4} x_n \right), \quad (9)$$

where $\chi_{v_n}(q_n)$ is the v_nth wave function of the high-frequency vibration and where $\varphi_{p_n}(x_n)$ is the p_nth wave function of the unperturbed low-frequency mode. The associated eigenvalues are expressed as

$$\epsilon(v_n,p_n) = \omega_0 v_n - A v_n(v_n-1) + \Omega(v_n)\left(p_n + \frac{1}{2} \right). \quad (10)$$

The meaning of Eqs. (9) and (10) can be understood as follows. When the high-frequency mode is in its ground state, i.e., $v_n=0$, both the local Hamiltonian H_n and its transformation under the dilatation operator $\hat{H}_n$ are identical. They describe the unperturbed low-frequency local mode whose eigenstates refer to a fixed number p_n of unperturbed phonons with frequency Ω_0. When v_n vibrons are created onto the nth site, the potential energy of the local mode is modified and a scaling of the local mode coordinate occurs. This scaling corresponds to a dilatation of the corresponding wave function [Eq. (9)] and to a frequency which depends on the vibron number [Eq. (10)]. However, a dilated state can be expressed as a superimposition of unperturbed phonon states (see Appendix A). Therefore, in a strong analogy with the standard polaron formalism, the dilatation of the phonon is equivalent to the occurrence of a virtual cloud of unperturbed phonons responsible for the dressing of the vibrons. This dressing modifies both the vibrational frequency and the anharmonic parameter of the high-frequency mode which, in turn, depend on the number of dilated phonons. For instance, when the nth site exhibits p_n dilated phonons, the fundamen-

tal frequency of the internal mode defined as $\omega_{01}=\epsilon(1,p_n)-\epsilon(0,p_n)$ is expressed as

$$\omega_{01}=\omega_0+\delta\omega\left(p_n+\tfrac{1}{2}\right), \tag{11}$$

where $\delta\omega=\Omega(1)-\Omega_0$. In the same way, the anharmonic parameter which accounts for the shift between $\omega_{01}=\epsilon(1,p_n)-\epsilon(0,p_n)$ and $\omega_{21}=\epsilon(2,p_n)-\epsilon(1,p_n)$ is written as

$$A'=A+\delta A\left(p_n+\tfrac{1}{2}\right), \tag{12}$$

where $\delta A=[2\Omega(1)-\Omega(2)-\Omega_0]/2$

B. Mean field procedure and effective Hamiltonian

When turning on the vibron hopping constant Φ, an exact diagonalization of the Hamiltonian H cannot be reached. Nevertheless, the vibron-phonon coupling can be partially removed by generalizing the previous procedure and by introducing the unitary transformation $U=\Pi_n U_n$. The transformed Hamiltonian is thus written as

$$\hat{H}=\sum_n \omega_0 b_n^\dagger b_n - A b_n^\dagger b_n^\dagger b_n b_n + \Omega(N_n)\left(\frac{p_n^2}{2}+\frac{x_n^2}{2}\right) + \Phi[\Theta_n^+\Theta_{n+1}^- b_n^\dagger b_{n+1} + \text{H.c.}], \tag{13}$$

where $\Theta_n^\pm$ is the dressed operator defined as

$$\Theta_n^\pm = e^{-[\theta(N_n)-\theta(N_n\mp 1)][(1/2)+ix_n p_n]}. \tag{14}$$

In this dressed vibron point of view [Eq. (13)], the nondiagonal vibron-phonon coupling remains through the modulation of the lateral terms by the dressing operators $\Theta_n^\pm$. These operators depend on the phonon coordinates in a highly nonlinear way and do not conserve the phonon numbers.

To overcome these difficulties, a mean field procedure is applied by following the small polaron theory.[29–37] To proceed, we take advantage of the fact that the optical phonons strongly interact with the phonons of the substrate which act as a thermal bath. As a result, when no vibron is excited in the nanowire, the unperturbed optical phonons are supposed to be in thermal equilibrium at the temperature T imposed by the substrate. In that context, the mean field procedure consists in substituting the vibron-phonon coupling terms occurring in Eq. (13) by their average values. As a result, the transformed Hamiltonian $\hat{H}$ is expressed as the sum of three separated contributions as

$$\hat{H}=\hat{H}_e+H_p+\Delta\hat{H}, \tag{15}$$

where $\hat{H}_e=\langle(\hat{H}-H_p)\rangle$ denotes the effective Hamiltonian of the dressed vibrons and where $\Delta H=\hat{H}-H_p-\langle(\hat{H}-H_p)\rangle$ stands for the remaining part of the vibron-phonon interaction. The symbol $\langle\ \rangle$ represents the thermal average over the unperturbed phonons. The effective dressed vibron Hamiltonian is written as

$$\hat{H}_e=\sum_n \omega_0 b_n^\dagger b_n - A b_n^{\dagger 2} b_n^2 + [\Omega(N_n)-\Omega_0]\left(n_B+\tfrac{1}{2}\right) + \Phi[\langle\Theta_n^+\Theta_{n+1}^-\rangle b_n^\dagger b_{n+1} + \text{H.c.}], \tag{16}$$

where $n_B=[\exp(\Omega_0/kT)-1]^{-1}$ is the Bose number. The remaining coupling term $\Delta\hat{H}$ is split into two contributions as

$$\Delta\hat{H}_1=\sum_n (\Omega(N_n)-\Omega_0)(a_n^\dagger a_n - n_B),$$

$$\Delta\hat{H}_2=\sum_n \Phi[(\Theta_n^+\Theta_{n+1}^- - \langle\Theta_n^+\Theta_{n+1}^-\rangle) b_n^\dagger b_{n+1} + \text{H.c.}]. \tag{17}$$

Within the mean field approach developed for the small polaron theory, the dynamics of the dressed vibrons is described by the effective Hamiltonian $\hat{H}_e$, only. The remaining vibron-phonon coupling $\Delta\hat{H}$ which is responsible for dephasing mechanisms, is usually addressed in a second step by using a standard perturbative theory. In the present problem, the situation differs slightly because although the remaining coupling $\Delta\hat{H}_2$ can be effectively neglected, the interaction $\Delta\hat{H}_1$ has to be included to describe the vibron dynamics.

To clarify this feature, let us take advantage of the small value of the vibron-phonon coupling when compared to the optical phonon frequency. Indeed, this assumption appears to be rather good for nanowires involving small molecules, since for CO/Ni, CO/Ru, and H/Si the ratio $|\Delta|/\Omega_0$ is estimated to be 0.17,[38–40] 0.12,[40–44] and 0.05,[45] respectively. Therefore, this approximation allows us to linearize Eq. (7) so that $\theta(N_n)\approx\Delta N_n/4\Omega_0$. The expansion of the dressing operators with respect to Δ clearly shows that $\Delta\hat{H}_2$ scales as $\Phi\Delta/\Omega_0$, whereas the interaction $\Delta\hat{H}_1$ is typically proportional to Δ. Consequently, the coupling $\Delta\hat{H}_2$ can be disregarded whereas $\Delta\hat{H}_1$, whose strength is typically of about the vibron hopping constant, must be conserved.

In the weak $|\Delta|/\Omega_0$ limit, the average value of the dressing operator $\langle\Theta_n^\pm\rangle$ reduces to a c number independent on the site position (see Appendix B). The effective Hamiltonian is thus characterized by an effective hopping constant for the dressed vibrons, $\hat{\Phi}=\Phi\langle\Theta_n^+\Theta_{n+1}^-\rangle$, expressed as

$$\hat{\Phi}=\frac{\Phi}{\sinh^2\left(\frac{\Delta}{8\Omega_0}\right)\coth^2\left(\frac{\Omega_0}{2kT}\right)+\cosh^2\left(\frac{\Delta}{8\Omega_0}\right)}. \tag{18}$$

Finally, the restriction to the two-vibron subspace is achieved by expanding the term $\Omega(b_n^\dagger b_n)$ in a normal ordering where, in each term of the expansion, all the creation operators are to the left of the annihilation operators. After some algebraic manipulations the effective dressed vibron Hamiltonian is written as

$$\hat{H}_e=\sum_n \hat{\omega}_0 b_n^\dagger b_n - \hat{A} b_n^{\dagger 2} b_n^2 + \hat{\Phi}[b_n^\dagger b_{n+1} + \text{H.c.}], \tag{19}$$

where $\hat{\omega}_0=\omega_0+\delta\omega\left(n_B+\frac{1}{2}\right)$ and $\hat{A}=A+\delta A\left(n_B+\frac{1}{2}\right)$ [see Eqs. (11) and (12)]. Then, by neglecting the remaining coupling ΔH_2, the transformed Hamiltonian is approximated as

$$\hat{H} \approx \hat{H}_e + H_p + \sum_n [\delta\omega b_n^\dagger b_n - \delta A b_n^{\dagger 2} b_n^2](a_n^\dagger a_n - n_B). \tag{20}$$

The Hamiltonian $\hat{H}_e$ [Eq. (19)] is the restriction to the two-vibron subspace of the effective Hamiltonian $\hat{H}_e$ [Eq. (16)] in the weak $|\Delta|/\Omega_0$ limit. The dressing effect, responsible for a shift of both the vibrational frequency and the anharmonic parameter, reduces the vibron hopping constant. The last term in Eq. (20) characterizes the remaining coupling ΔH_1 which accounts for the fact that both the vibrational frequency and the anharmonic parameter of each admolecule depends on the number of dilated phonons (see Sec. III A).

C. The random lattice model for the vibron dynamics

As shown in the previous section, the vibron-phonon dynamics in the weak $|\Delta|/\Omega_0$ limit is described by the Hamiltonian Eq. (20) in which the knowledge allows us to compute, in principle, any observable. In practice, we are interested in the characterization of the vibron response to a given external excitation which usually involves a specific correlation function between vibron operators.[46] To compute such a response function, it is necessary to account for the fact that the optical phonons are in thermal equilibrium at temperature T. Therefore, a statistical average has to be realized according to the initial density matrix ρ_p defined as

$$\rho_p = \frac{e^{-H_p/kT}}{\mathrm{Tr}(e^{-H_p/kT})}. \tag{21}$$

These calculations are greatly simplified since the Hamiltonian $\hat{H}$ [Eq. (20)] is block diagonal in the basis formed by the eigenstates $|p_1, p_2, \ldots, p_n, \ldots,\rangle$ of the unperturbed phonon Hamiltonian H_p. Therefore, when the phonons are in a particular eigenstate $|p_1, p_2, \ldots, p_n \ldots,\rangle$, the vibron dynamics is described by the Hamiltonian [see Eq. (20)]

$$\hat{h}(\{p_n\}) = \hat{H}_e + \sum_n [\delta\omega b_n^\dagger b_n - \delta A b_n^{\dagger 2} b_n^2](p_n - n_B). \tag{22}$$

By solving Eq. (22), the required observable can be easily determined for a given configuration of the phonon numbers. Then, the thermal average is achieved by performing a statistics over the different phonon eigenstates according to the Boltzmann density matrix Eq. (21).

Consequently, Eq. (22) clearly shows that the vibron dynamics in the nanowire is equivalent to the dynamics in a disordered lattice in which both the frequencies and the anharmonicities of the admolecules are inhomogeneously distributed. These dynamical parameters depend on the number of dilated phonons $\{p_n\}$ which can be viewed as a set of independent random variables distributed according to the geometric law [see Eq. (21)]

$$P(p_n) = \left[1 - \exp\left(-\frac{\Omega_0}{kT}\right)\right] \exp\left(-\frac{\Omega_0 p_n}{kT}\right). \tag{23}$$

Therefore, averaging over the phonon bath is equivalent to perform the average over a frozen disorder whose realization is specified by the set of phonon numbers.

The following section is thus devoted to a numerical analysis of the random Hamiltonian Eq. (22) with a special emphasis on the influence of the disorder on the TVBS.

IV. NUMERICAL RESULTS

In this section, the random Hamiltonian Eq. (22) is diagonalized to characterize the two-vibron states of the adsorbed nanowire. The diagonalization is achieved by using the number state method,[26] which was successfully applied to molecular adsorbates.[2–6] Within this method, the two-vibron eigenstate is expanded as

$$|\Psi_\alpha\rangle = \sum_{n_1, n_2 \geqslant n_1} \Psi_\alpha(n_1, n_2)|n_1, n_2), \tag{24}$$

where $\{|n_1, n_2)\}$ denotes a local basis set normalized and symmetrized according to the restriction $n_2 \geqslant n_1$ due to the indistinguishable nature of the vibrons. A particular vector $|n_1, n_2)$ characterizes two vibrons located onto the sites n_1 and n_2, respectively.

When the disordered nature of Eq. (22) is disregarded, i.e., when we restrict our attention to the effective vibron Hamiltonian $\hat{H}_e$, the diagonalization is simplified by taking advantage of the lattice periodicity. Indeed, the two-vibron wave function is invariant with respect to a translation along the lattice and it can be expanded as a Bloch wave as

$$\Psi_\alpha(n_1, n_1 + m) = \frac{1}{\sqrt{N}} \sum_{n_1} e^{ik(n_1 + m/2)} \Psi_{\alpha,k}(m), \tag{25}$$

where the momentum k, which belongs to the first Brillouin zone of the molecular lattice, is associated with the motion of the center of mass of the two vibrons. The resulting wave function $\Psi_{\alpha,k}(m)$ refers to the degree of freedom m which characterizes the distance between the two vibrons. Since k is a good quantum number, the effective Hamiltonian is block diagonal and the Schrödinger equation can be solved for each k value.

The two-vibron energy spectrum of the effective Hamiltonian $\hat{H}_e$ [Eq. (19)] is shown in Fig. 2 for $\Phi = 4\ \mathrm{cm}^{-1}$, $A = 15\ \mathrm{cm}^{-1}$, $\Omega_0 = 50\ \mathrm{cm}^{-1}$, and $\Delta = -6\ \mathrm{cm}^{-1}$. This spectrum, centered onto the frequency $2\omega_0$, exibits the two-vibron dispersion curves drawn in the first Brillouin zone of the lattice. When $T = 100$ K [Fig. 2(a)], the spectrum is formed by an energy continuum symmetrically located around $2\hat{\omega}_0$ which is redshifted of about $8.97\ \mathrm{cm}^{-1}$ from $2\omega_0$. The TVFS bandwidth is equal to $31.89\ \mathrm{cm}^{-1}$. This continuum contains the states describing two independent vibrons and called TVFS. The energy spectrum shows a single band located below the continuum over the entire Brillouin zone. This band contains the TVBS which describe two vibrons trapped around the same site and which the center of mass propagates with a wave vector k. The binding energy of TVBS, i.e., the gap

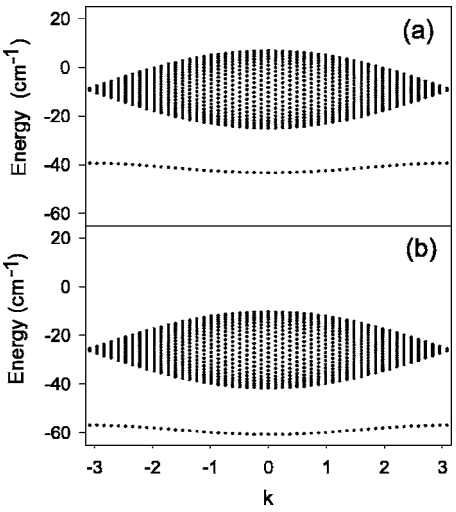

FIG. 2. Two-vibron energy spectrum for $\Phi=4$ cm^{-1}, $A=15$ cm^{-1}, $\Omega_0=50$ cm^{-1}, $\Delta=-6$ cm^{-1}; (a) $T=100$ K and (b) $T=300$ K.

between the zero wave vector TVBS and the bottom of the TVFS continuum, is equal to 18.33 cm^{-1}, whereas its bandwidth is about 3.94 cm^{-1}.

When $T=300$ K [Fig. 2(b)], the spectrum displays the same features as observed in Fig. 2(a). However, the main difference is a strong redshift of both the TVFS continuum and the TVBS. Indeed, the continuum is centered around $2\hat{\omega}_0$ which is now redshifted of about 25.94 cm^{-1} from $2\omega_0$. The TVFS bandwidth has been slightly reduced to 31.45 cm^{-1}. The binding energy of TVBS is equal to 18.98 cm^{-1}, whereas its bandwidth is equal to 3.78 cm^{-1}.

The influence of the temperature on the two-vibron energy spectrum can be understood from the knowledge of the behavior of the dynamical parameters which govern the vibron dynamics. This statement is illustrated in Fig. 3 which displays the temperature dependence of the effective hopping constant $\hat{\Phi}$ [Fig. 3(a)], of the frequency shift $\delta\omega$ [Fig. 3(b)] and of the anharmonicity shift δA [Fig. 3(c)]. The parameters are $\Phi=4$ cm^{-1}, $A=15$ cm^{-1}, $\Omega_0=50$ cm^{-1}, $\Delta=-6$ cm^{-1} (full line), $\Delta=-10$ cm^{-1} (dashed line), and $\Delta=6$ cm^{-1} (dotted line). As shown in Fig. 3(a), $\hat{\Phi}$ decreases with the temperature as in the standard small polaron formalism. It depends quadratical on the vibron-phonon coupling parameter Δ and it decreases as $|\Delta|$ increases. Nevertheless, due to the small value of the ratio $|\Delta|/\Omega_0$, $\hat{\Phi}$ exhibits a very small temperature dependence. For instance, when $\Delta=\pm 6$ cm^{-1}, it varies from $\hat{\Phi}=3.99$ cm^{-1} when $T=3$ K to $\hat{\Phi}=3.93$ cm^{-1} when $T=300$ K. By contrast, the frequency shift $\delta\omega$ strongly depends on the temperature and on the sign of Δ. It produces a blueshift for positive Δ values and a redshift for negative Δ values. For instance, when $\Delta=-6$ cm^{-1}, $\delta\omega$ varies from -4.48 cm^{-1} when $T=100$ K to -12.97 cm^{-1} when $T=300$ K. As shown in Fig. 3(c), the anharmonicity shift increases with the temperature whatever the sign of the vibron-phonon coupling Δ but it does not depend on the absolute value of Δ. For small $|\Delta|$ values, the anharmonicity shift is rather small since it varies from 0.16 cm^{-1} when $T=100$ K to 0.45 cm^{-1} when $T=300$ K for $\Delta=-6$ cm^{-1}. Nevertheless, stronger Δ value produces a more important shift.

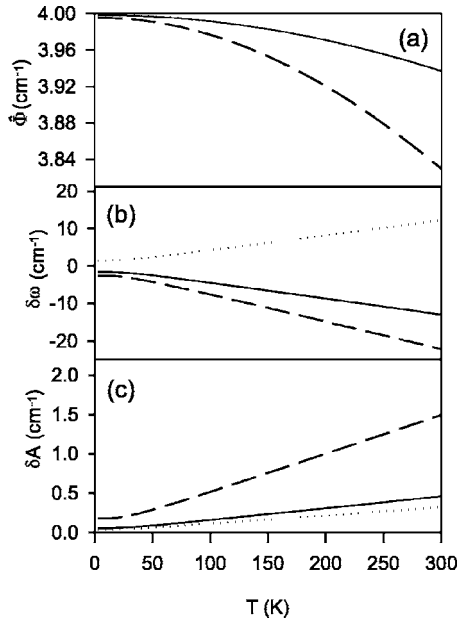

FIG. 3. Temperature dependence of (a) the effective vibron hopping constant $\hat{\Phi}$, (b) the vibron frequency shift, and (c) the vibron anharmonicity shift for $\Phi=4$ cm^{-1}, $A=15$ cm^{-1}, $\Omega_0=50$ cm^{-1}, $\Delta=-6$ cm^{-1} (full line), $\Delta=-10$ cm^{-1} (dashed line), and $\Delta=6$ cm^{-1} (dotted line).

In Fig. 4, the behavior of the zero wave vector TVBS frequency [Fig. 4(a)], of the TVBS binding energy [Fig. 4(b)] and of the TVBS bandwidth [Fig. 4(c)] is shown for the same set of parameters as in Fig. 3. The temperature dependence of the zero wave vector TVBS frequency is essentially

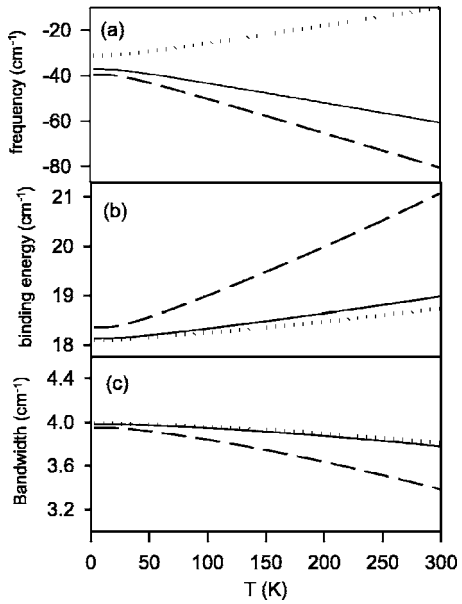

FIG. 4. Temperature dependence of (a) the zero wave vector TVBS frequency, (b) the TVBS binding energy and (c) the TVBS bandwidth for $\Phi=4$ cm^{-1}, $A=15$ cm^{-1}, $\Omega_0=50$ cm^{-1}, $\Delta=-6$ cm^{-1} (full line), $\Delta=-10$ cm^{-1} (dashed line) and $\Delta=6$ cm^{-1} (dotted line).

due to its strong depends on the frequency shift $\delta\omega$ [see Fig. 3(b)]. As a result, the bottom of the TVBS band is redshifted for negative Δ values whereas it is blueshifted for positive Δ values. By contrast, both the TVBS binding energy and the TVBS bandwidth exhibit a rather small temperature dependence. Whatever the sign of the vibron-phonon coupling Δ, the binding energy increases with the temperature whereas the bandwidth decreases with the temperature.

Let us now consider the nature of the two-vibron eigenstates connected to the random Hamiltonian Eq. (22). Note that to simplify the discussion, we shall restrict our attention to negative Δ values, only. As mentioned previously, this Hamiltonian describes the dynamics of two vibrons moving on a disordered lattice characterized by a set of random frequencies and random anharmonic parameters. From the standard localization theory, it is well known that the main consequence of randomness is the occurrence of localized states. As discussed in numerous papers (see, for instance, Refs. 47–49), a way to discriminate between localized or extended states is based on the analysis of the corresponding inverse participation ratio (IPR). In terms of the αth wave function $\Psi_\alpha(n_1,n_2)$, the IPR is defined as

$$I_\alpha = \sum_{n_1,n_2} |\Psi_\alpha(n_1,n_2)|^4. \tag{26}$$

In an ordered lattice extended states are characterized by an infinitesimally small IPR whereas, in a disorder lattice, the IPR of strongly localized states is close to unity.

In addition to the IPR, a useful quantity to analyze the two-vibron states is the mean value $\langle m_\alpha \rangle$ of the separating distance between two vibrons. For the αth eigenstate, it is defined as

$$\langle m_\alpha \rangle = \sum_{n_1,n_2} (n_2 - n_1)|\Psi_\alpha(n_1,n_2)|^2. \tag{27}$$

A small $\langle m_\alpha \rangle$ value indicates that the state refers to two trapped vibrons whereas large $\langle m_\alpha \rangle$ values characterize vibrons far from each other.

Figure 5 shows the IPR [Fig. 5(a)] and the mean separating distance [Fig. 5(b)] for each two-vibron eigenenergy centered around $2\hat{\omega}_0$. The lattice size is fixed to $N=51$ and the parameters are $\Phi=3$ cm^{-1}, $A=15$ cm^{-1}, $\Omega_0=50$ cm^{-1}, $\Delta=-4$ cm^{-1}, and $T=50$ K. To simplify the presentation, only five random configurations have been reported on the figures. The figures clearly discriminate between two kinds of states. As shown in Fig. 5(a), a set of states form an energy continuum located around $2\hat{\omega}_0$. These states are characterized by a rather weak IPR smaller than 0.2. Moreover, the separating distance between two vibrons varies typically between 5 and 40 which indicates that these states refer to two vibrons far from each other [Fig. 5(b)]. Consequently, the continuum contains the TVFS which are slightly perturbed by the disorder. Note that the most important IRP values occur at the center and at the edges of the continuum.

Below the continuum, several bands take place. All these bands contain states in which the two vibrons are trapped close to each other [Fig. 5(b)]. The first band, located around $-2\hat{\omega}_0-2\hat{A}$, corresponds to the TVBS of the effective Hamiltonian modified by the randomness. Figure 5(a) clearly shows that most of the TVBS have an IPR lower than 0.5 so that they appear more sensitive to the disorder than the TVFS. In addition, some TVBS are characterized by a strong IPR, close to 0.9, and they thus refer to strongly localized states.

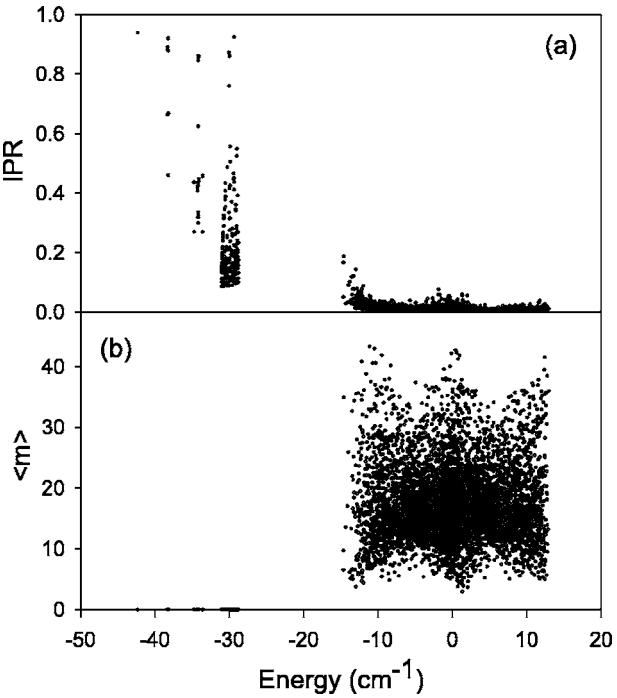

FIG. 5. (a) IPR and (b) mean separating distance for $N=51$, $\Phi=3$ cm^{-1}, $A=15$ cm^{-1}, $\Omega_0=50$ cm^{-1}, $\Delta=-4$ cm^{-1}, and $T=50$ K.

The next band, which is redshifted of about Δ from the TVBS band, contain bound states strongly localized. Because they lie around the energy $-2\hat{\omega}_0-2\hat{A}-2\delta\omega$, they correspond to two trapped vibrons localized on a site where a single dilated phonon has been thermally excited. However, the occurrence of several eigenenergies, i.e., a nonvanishing bandwidth, is the signature of the presence of clusters involving two dilated phonons located onto two nearest neighbor sites. The following bands, which are shifted of about 2Δ and 3Δ from the TVBS band, describe two trapped vibrons localized onto sites containing successively two dilated phonons and three dilated phonons. The strong IPR values indicate that these states are strongly localized. Note that for this small temperature, the probability for the excitation of more than one dilated phonon is relatively weak so that these bands do not contain a lot of states.

The influence of the temperature is illustrated in Fig. 6 where $T=150$ K. The other parameters are equal to those used in Fig. 5. In that case, the TVFS experience a strong perturbation since most of them are characterized by an important IPR value. Nevertheless, a lot of states with a small IPR value remain, especially close to the band center. In fact, the strongly perturbed states are redshifted from the center of the band and lie in the frequency range of both the TVBS band and the following bands. Nevertheless, since these states refer to vibrons localized far from each other, they do

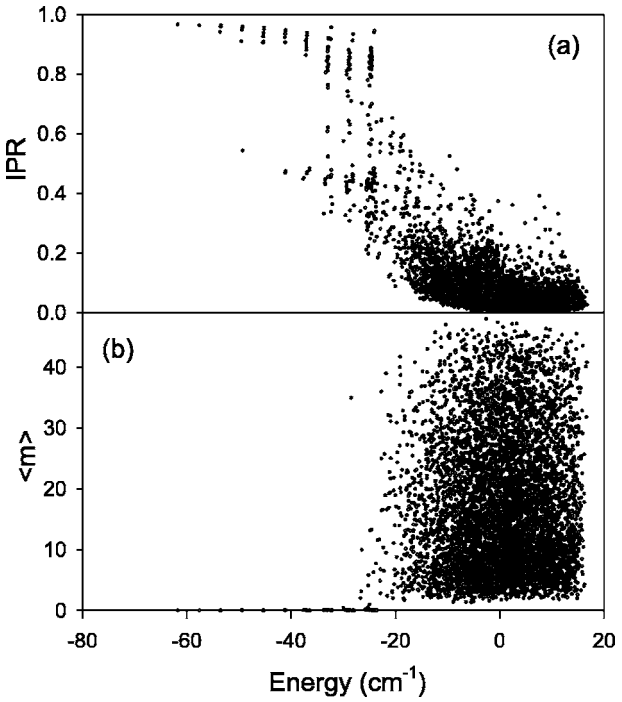

FIG. 6. (a) IPR and (b) mean separating distance for $N=51$, $\Phi=3$ cm^{-1}, $A=15$ cm^{-1}, $\Omega_0=50$ cm^{-1}, $\Delta=-4$ cm^{-1}, and $T=150$ K.

not interfere with bound states. For the bound states, the main difference with the situation illustrated in Fig. 5 is an increase of the IPR which corresponds to an enhancement of the localization. In addition, the figure clearly shows the occurrence of several bands which refer to trapped vibrons localized onto sites where a large number of dilated phonons is excited. Note that the TVBS binding energy exhibits a blushifted when compared to the situation illustrated in Fig. 5.

Let us now focus our attention on the nature of the TVBS. In Fig. 7, the wave function $\Psi_\alpha(n_1,n_1)$ of the first 21 states belonging to the TVBS band has been reported. For this simulation, the parameters are $\Phi=3$ cm^{-1}, $A=12$ cm^{-1}, $\Omega_0=50$ cm^{-1}, $\Delta=-4$ cm^{-1}, and $T=50$ K. The lattice size is fixed to $N=61$ and a single random configuration has been considered. The corresponding distribution of the dilated phonons is shown in the bottom of the figure where an open circle, a full circle, and a full gray square account for the occurrence of zero, one, and two dilated phonons, respectively. Note that starting from the bottom of the figure, the wave functions are plotted according to an increase of their energy. The figure shows that the TVBS wave functions are localized at nonoverlapping segments. Some of these wave functions can be grouped into local sets involving states localized on the same segment. For each set, the wave functions are similar to those of a single particle confined in a box. They have an almost perfect symmetry and the number of nodes increases with the energy. The confinement takes place between two sites which contain a nonvanishing number of dilated phonons. For instance, such a situation occurs for the segment confined between the sites 11 and 21. By contrast, other states are not strictly confined between two defects but extend over a segment which contain sites where dilated phonons are excited. This situation takes place between the sites 26 and 46.

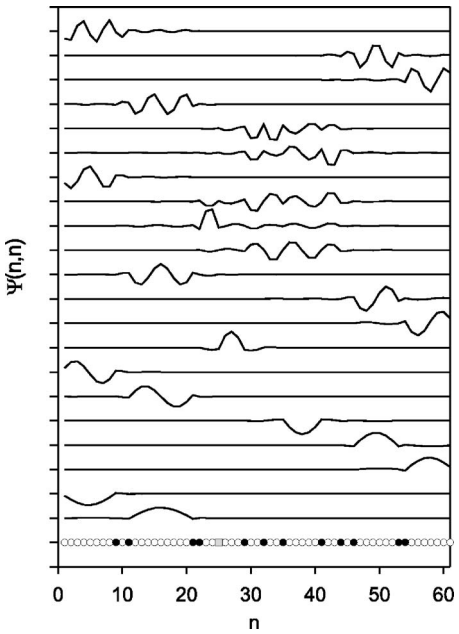

FIG. 7. The first 21 TVBS wave functions for $N=61$, $\Phi=3$ cm^{-1}, $A=12$ cm^{-1}, $\Omega_0=50$ cm^{-1}, $\Delta=-4$ cm^{-1}, and $T=50$ K. The corresponding phonon distribution is shown in the bottom of the figure where an open circle, a full circle, and a full gray square account for the occurrence of zero, one, and two dilated phonons, respectively.

At this step, to perform a more efficient average over a large number of random configurations, let us consider the following procedure to analyze the TVBS dynamics. For molecular adsorbates the intramolecular anharmonicity is usually stronger than the vibron hopping constant. Therefore, the mean separating distance between two vibrons in a bound state almost vanishes (see Figs. 4 and 5) so that two trapped vibrons can be viewed as a single particle. The dynamics of that particle is well represented by considering the reduction of the full Hamiltonian to the subspace generated by the basis set $|n\rangle \equiv |n,n\rangle$. Consequently, from Eqs. (19) and (22), this reduced Hamiltonian is expressed as

$$h_{TVBS} = \sum_n \epsilon_n |n\rangle\langle n| - \frac{\hat{\Phi}^2}{\hat{A}}(|n\rangle\langle n+1| + \text{H.c.}), \qquad (28)$$

where the energy for a vibron pair located on the nth site is a random variable defined as

$$\epsilon_n = 2\left(\hat{\omega}_0 - \hat{A} - \frac{\hat{\Phi}^2}{\hat{A}} + (\delta\omega - \delta A)(p_n - n_B)\right) \qquad (29)$$

and where $\hat{\Phi}^2/\hat{A}$ is the effective vibron pair hopping constant.[6] It describes the transtion amplitude for the pair to realize a hop from the state $|n,n\rangle$ to the state $|n+1,n+1\rangle$ via $|n,n+1\rangle$. Within this approach, the dimension of h_{TVBS}, equal to the number of sites N, has been strongly reduced when compared to the dimension of the full two-vibron subspaces equal to $N(N+1)/2$.

Figure 8 shows a detailed analysis of the TVBS IPR in a lattice containing $N=200$ sites and for 40 random configura-

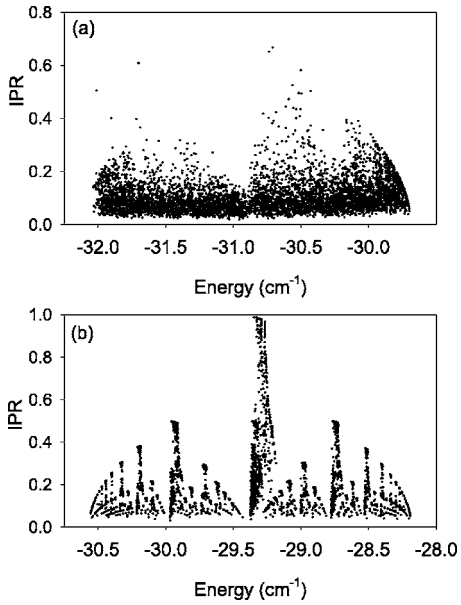

FIG. 8. IPR of the TVBS for 40 random configurations and for $N=200$, $\Phi=3$ cm^{-1}, $A=15$ cm^{-1}, $\Omega_0=50$ cm^{-1}, and $T=50$ K. (a) $\Delta=-1$ cm^{-1} and (b) $\Delta=-6$ cm^{-1}.

tions. The parameters are $\Phi=3$ cm^{-1}, $A=15$ cm^{-1}, $\Omega_0=50$ cm^{-1}, and $T=50$ K. For $\Delta=-1$ cm^{-1} [Fig. 8(a)], most of the TVBS appear weakly perturbed by the disorder and are characterized by an IPR lower than 0.2. These states are uniformly distributed in the band. Nevertheless, the lattice supports states with a rather large IPR which ranges between 0.2 and 0.9. When $\Delta=-6$ cm^{-1} [Fig. 8(b)], the IPR of the TVBS behave differently. The figure clearly shows a kind of structure symmetrical distributed around the center of the band in which the eigenenergies are condensed into local groups. Each group is characterized by a given maximum value of the IPR. For instance, the group located at the center of the band contains states which the IPR ranges between 0 and 1. Then two groups, characterized by a maximum IRP equal to 0.5, are, respectively, redshifted and blueshifted of about 0.6 cm^{-1} from the center of the band. Note that this shift is about the hopping constant $\hat{\Phi}^2/\hat{A}$ of the vibron pair.

This behavior clearly indicates the occurrence of a transition which discriminates between two kind of TVBS depending on the strength of the vibron-phonon coupling.

In Fig. 9, the behavior of the distribution $P(I)$ of the IPR of the TVBS is illustrated for $\Phi=3$ cm^{-1}, $A=15$ cm^{-1}, and $\Omega_0=50$ cm^{-1} and for two values of the vibron-phonon coupling equal to $\Delta=-1$ cm^{-1} and $\Delta=-6$ cm^{-1}, respectively. Three temperatures have been considered, i.e., $T=40$ K [Fig. 9(a)], $T=100$ K [Fig. 9(b)] and $T=200$ K [Fig. 9(c)]. To build the distribution, we use a lattice formed by $N=200$ sites and 400 random configurations were accumulated. At low temperature and weak vibron-phonon coupling [Fig. 9(a)], the IPR exhibits a continuous distribution which is maximum for $I=0.05$ and which decreases exponentially for large IPR values. For $\Delta=-6$ cm^{-1}, the shape of the distribution slightly changes. It appears almost continuous for small IPR values and it reaches a maximum for $I=0.08$. Then, it decreases by exhibiting a structure characterized by peaks

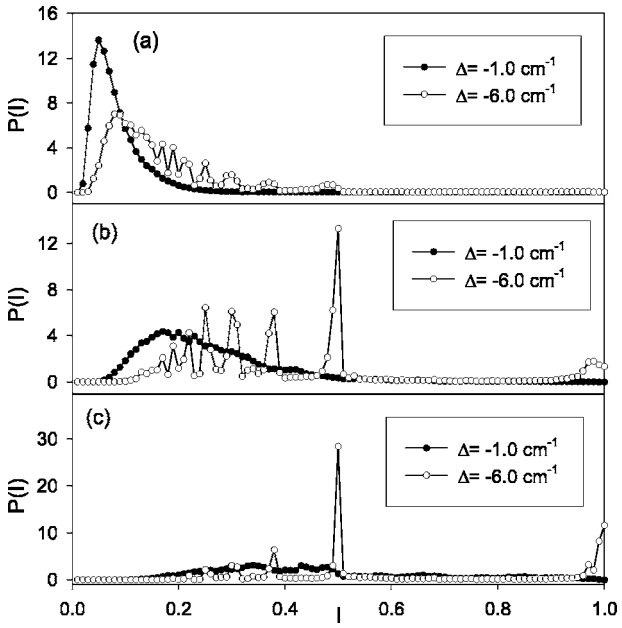

FIG. 9. Distribution of the TVBS IPR for $N=200$, $\Phi=3$ cm^{-1}, $A=15$ cm^{-1}, $\Omega_0=50$ cm^{-1}. $\Delta=-1$ cm^{-1} (full circles), and $\Delta=-6$ cm^{-1} (open circles). (a) $T=40$ K, (b) $T=100$ K, and (c $T=200$ K.

with small amplitudes. At $T=100$ K [Fig. 9(b)], the IPR distribution is always continuous for $\Delta=-1$ cm^{-1} but its maximum occurs for $I=0.17$. By contrast, when $\Delta=-6$ cm^{-1}, the continuous nature of the distribution has clearly disappeared. It is formed by peaks where the most intense is located at $I=0.5$. Finally, when $T=200$ K [Fig. 9(c)], the continuous nature of the IPR distribution for a weak vibron-phonon coupling remains although some small amplitude oscillations occur. The maximum of the distribution takes place for $I=0.34$. For a strong vibron-phonon coupling, the distribution exhibits six peaks which the most intense occurs for $I=0.5$.

Finally, Fig. 10 shows the behavior of the average IPR of the TVBS as a function of Δ for $T=40$ K, $T=100$ K, $T=200$ K, and $T=300$ K. The parameters are those used in Fig. 9. Whatever the temperature, the average IPR exhibits two regimes depending on the strength of the vibron-phonon

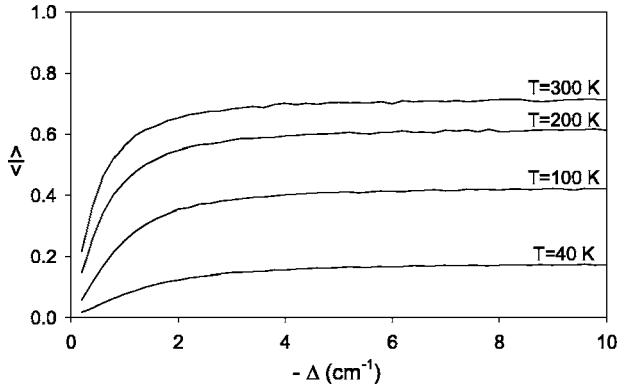

FIG. 10. Average TVBS IPR for $N=200$, $\Phi=3$ cm^{-1}, $A=15$ cm^{-1}, and $\Omega_0=50$ cm^{-1} as a function of Δ for $T=40$ K, $T=100$ K, $T=200$ K, and $T=300$ K.

coupling. For small $|\Delta|$ values, it increases with $|\Delta|$ according to a linear law. Then, above a critical value, the average IPR becomes almost independent on the vibron-phonon coupling and it reaches a constant value. This constant value strongly depends on the temperature and it increases as the temperature increases. Note that the critical value decreases with the temperature. In other words, below a critical value, both the vibron-phonon coupling and the temperature are responsible for an enhancement of the TVBS localization. By contrast, above the critical value, the vibron-phonon coupling does not significantly affect the localized nature of the TVBS. Nevertheless, the localization still depends on the temperature which, as previously, enhances the localization.

V. DISCUSSION

Within the standard small polaron approach, the linear dependence of the vibron-phonon coupling with respect to the low-frequency mode coordinates leads to the occurrence of a lattice distortion on the site where the vibrons have been created. In an adsorbed nanowire, we have shown that the quadratic dependence of the vibron-phonon coupling with the local mode coordinates favors a fully different dressing mechanism. Indeed, when no vibron is excited, each lattice site is occupied by a local mode whose eigenstates are described by unperturbed phonons. The creation of one or two vibrons on the nth site is thus responsible for the scaling of the coordinate and for the dilation of the wave function of the nth local mode. Since a dilated state corresponds to a superimposition of unperturbed phonons, a virtual cloud of phonons accompanies the creation of the vibrons. This dressing manifests itself by a dependence on the phonon numbers of the dynamical parameters (internal frequency and intramolecular anharmonicity) which govern the vibron dynamics.

Because the low-frequency modes are assumed to be in thermal equilibrium due to thier coupling with the phonons of the substrate, we applied a mean field procedure and we defined an effective Hamiltonian $\hat{H}_e$ [Eq. (19)] for the dressed vibrons by fixing the number of dilated phonons to their average value. In that case, as shown in Figs. 1–3, the properties of the bound states depend on both the temperature and the vibron-phonon coupling Δ. More precisely, it has been shown that the TVBS band exhibits a strong frequency shift with the temperature. Negative Δ values induce a redshift whereas a blueshift takes place for positive Δ values. This behavior originates in the frequency shift $\omega_0 \rightarrow \omega_0 + \delta\omega\left(n_B + \frac{1}{2}\right)$ experienced by each high-frequency mode due to the dressing mechanism. Because the vibron-phonon coupling strength is usually smaller than the phonon frequency, this shift is proportional to the vibron-phonon coupling and it scales as $\delta\omega \approx \Delta$ [see Eq. (11)]. By contrast, both the TVBS binding energy and the TVBS bandwidth do not significantly change with the temperature. The weak temperature dependence of the TVBS binding energy results from the small modification of the intramolecular anharmonicity for the dressed admolecules. Indeed, the dressing induces a shift $\delta A\left(n_B + \frac{1}{2}\right)$ of the anharmonic parameter [see Eq. (12)] governed by the constant $\delta A \approx \Delta^2/8\Omega_0$. In the same way, at the lowest order with respect to Δ/Ω_0, the correction of the effective hopping constant scales as $\Phi(\Delta/\Omega_0)^2$ so that it yields rather small modifications of the TVBS bandwidth with respect to that occurring for undressed bound states.

These features clearly indicate that the present dressing mechanism is rather different than the dressing experienced by the vibrons described within the small polaron formalism. Indeed, in this latter case, a similar redshift affects both the frequency and the anharmonicity of each molecule. This redshift is given by the so-called small polaron binding energy which is temperature independent and proportional to the square of the vibron-phonon coupling. By contrast, in the small polaron model, the effective hopping constant is drastically modified and it strongly decreases with the temperature.

The remaining coupling between the dressed vibrons and the dilated phonons account for the thermal fluctuations of the number of dilated phonons. This coupling results in a vibron Hamiltonian equivalent to the Hamiltonian of a disordered lattice in which both the frequency and the anharmonicity of the admolecules are inhomogeneously distributed. These parameters depend on the phonon numbers which form a set of independent random variables. In one dimension, it is well known that this kind of Hamiltonian leads to the localization of the vibron states. By localization, it is meant that disorder can trap the vibrons by quantum interference to a finite region so that all the states turned out to be localized, even if the disorder is infinitesimally small.

To discuss and interpret our numerical results, let us focus our attention on the influence of the disorder on the TVBS, only. The ideal lattice is obtained when no phonon is excited so that all the sites are equivalent. The randomness occurs when defects take place on the different sites. A particular defect corresponds to a site on which the number of phonons p_n does not vanish. Consequently, on this site, both the frequency and the anharmonicity of the corresponding admolecule are shifted from their value in the ideal lattice.

When a single defect is present, the lattice supports a localized TVBS which refer to two trapped vibrons localized around the defect. The energy of this state depends on the number of excited phonons and it is shifted from the TVBS band of about $2(\delta\omega - \delta A)p_n \approx \Delta p_n$. When several defects occur, some of them can form clusters corresponding to defects located onto nearest neighbor sites. If in a given cluster all the sites exhibit the same number of phonons, the different localized states hybridize to form a finite bandwidth band called an impurity band. Since the number of phonons follows the Boltzmann distribution, the temperature control the number of phonons as well as the size of the clusters. Therefore, at low temperature, the lattice essentially supports a dilute set of defects containing a small number of phonons. We thus observe the occurrence of a few impurity bands with basically zero bandwidth. By contrast, when the temperature increases, the number of phonons per defect increases as well as the size of the clusters. Consequently, several impurity bands take place with a significant bandwidth.

In addition to create impurity bands, the disorder strongly affects the TVBS described by the effective Hamiltonian. When compared with the standard localization theory, we observed the occurrence of a transition which discriminates

between two kinds of localization depending on the strength of vibron-phonon coupling. As mentioned in Sec. IV these features were pointed out through the study of the IPR which allows us to discriminate between localized or extended states. In an ordered lattice extended states are characterized by an infinitesimally small IPR whereas, in a disorder lattice, the IPR of strongly localized states is close to unity.

For small $|\Delta|$ values, most of the TVBS are weakly perturbed by the disorder. They are characterized by a rather small IPR value and they are almost uniformly distributed in the TVBS band. Nevertheless, the lattice supports some strongly localized states whose IPR is close to unity [Fig. 8(a)]. Consequently, the distribution of the IPR is continuous. It is peaked around a rather small IPR value and falls off exponentially for large IPR values (Fig. 9). In fact, this specific behavior of the IPR distribution exhibits a universal character which has been determined in previous theoretical works.[50,51] Indeed, from Fig. 9, it is straightforward to show that the continuous distribution is well reproduced by the following universal expression:

$$P(I) = 4\pi^2\xi\sum_{j=1}^{\infty}(4\pi^2 j^4 I\xi - 3j^2)\exp(-2\pi^2 j^2 I\xi), \quad (30)$$

where ξ denotes an effective localization length. This universal behavior indicates that the localization of the TVBS results form the quantum interferences which originate in the scattering of the TVBS by the inhomogeneous defect distribution. From Eq. (30), the average value of the IPR is expressed in terms of the effective localization length as $\langle I\rangle = 1/6\xi$. As shown in Fig. 10, the average IPR increases linearly with $|\Delta|$ for small vibron-phonon coupling. This behavior depends on the temperature and a fit of the numerical data allows us to determine the expression of $\langle I\rangle$ in terms of both the temperature and the hopping constant for bound states. As a result, the effective localization length is approximately expressed as

$$\xi \approx 0.92\frac{\Omega_0}{kT}\frac{\hat{\Phi}^2}{\hat{A}|\Delta|}. \quad (31)$$

The decrease of the localization length with both the temperature and the vibron-phonon coupling results from the enhancement of the disordered nature of the lattice. By contrast, the breatherlike behavior of the bound states manifests itself by an increase of the localization because the anharmonicity prevents the propagation of the vibron pair.

For strong values of the vibron-phonon coupling strength, the IPR of the TVBS form a structure symmetrical distributed around the center of the band in which the eigenenergies are condensed into local groups. Each group is characterized by a given maximum value of the IPR [Fig. 8(b)] and the corresponding IPR distribution exhibits a discrete character involving several peaks (Fig. 9). Finally, the average IPR appears almost independent on the vibron-phonon coupling but it increases with the temperature. To interpret these features, let us mention that for a strong vibron-phonon coupling each defect in the lattice behaves as an infinite potential barrier which prevents the propagation of the vibron pair. Consequently, for a given defect distribution, the lattice exhibits a set of clusters free from defects. A given cluster, characterized by its size L, is formed by a set of L nearest neighbor sites without defect. Such a cluster is thus responsible for the confinement of the vibron pair which behaves as a single particle confined in a box. In that case, the TVBS are the eigenstates of the confined pair.

From the TVBS reduced Hamiltonian [Eq. (28)], it is straightforward to show that the eigenenergies for a pair confined in a cluster with size L are defined as

$$\omega_p(L) = \epsilon_0 - 2\frac{\hat{\Phi}^2}{\hat{A}}\cos\left(\frac{p\pi}{L+1}\right), \quad (32)$$

where $p=1,\ldots,L$ and where $\epsilon_0=\langle\epsilon_n\rangle$. The corresponding eigenfunctions are stationnary states written as

$$\Psi_{p,L}(n) = \sqrt{\frac{2}{L+1}}\sin\left(\frac{p\pi n}{L+1}\right). \quad (33)$$

For these eigenstates localized in a region of size L, the IPR is defined as

$$I_p(L) = \frac{1.5}{L+1} + \frac{0.5}{L+1}\delta_{p,(L+1)/2}. \quad (34)$$

These set of equations allows us to reproduce the behavior observed in Fig. 8(b). Indeed, for each L values, the states corresponding to $p=(L+1)/2$ are located in the center of the TVBS band. They are characterized by an IPR equal to $1/(L+1)$ which varies from 1 for $L=1$ to zero for L tends to infinity. All these values of the IPR are condensed in the central peak observed in Fig. 8(b). Then, the energy of the states corresponding to $p=(L+1)/3$ are shifted from the central peak of about $\hat{\Phi}^2/\hat{A}$. They are characterized by an IPR equal to $1.5/(L+1)$ which varies from 0.5 for $L=2$ to zero for L tends to infinity. This procedure allows us to reproduce all the features observed in Fig. 8(b). Consequently, in this strong vibron-phonon coupling regime, the TVBS correspond to all the possible combinations for stationary states confined on clusters of different sizes. However, each configuration does not occur with the same probability since the temperature controls both the number of clusters and the value of their size. From the standard percolation theory, the probability for the occurrence of a cluster of size L free from defect, i.e., free form dilated phonons, is defined as $\wp(L) = L(1-Q)^2Q^{L-1}$, where $Q=1-\exp(-\Omega_0/kT)$ is the probability for a site to be free from defect. The different observations are thus weighted by the distribution $\wp(L)$. In particular the average value of the IPR defined as $\langle I\rangle = \Sigma_{L=1}^{\infty}\Sigma_{p=1}^{L}\wp(L)I_p(L)/L$ is written as

$$\langle I\rangle = \frac{3}{2}\frac{1-Q}{Q} + \frac{(1-Q)^2}{6Q^2}\ln\left(\frac{(1-Q)^5}{1+Q}\right). \quad (35)$$

Equation (35) reproduces the behavior of the average IPR which appears independent on the vibron-phonon coupling. As observed in Fig. 10, it increases with the temperature and behaves as $\langle I\rangle \approx 1-Q$ when Q tends to zero, i.e. when $kT \gg \Omega_0$.

These results clearly establish the occurrence of a transition between two kinds of localization. For small $|\Delta|$ values, the localization of the TVBS results from quantum interferences and it follows a universal behavior. By contrast, for strong $|\Delta|$ values, the localization originates in the occurrence of inifinite potential barriers which confine the vibron pair onto clusters whose both number and size are controlled by the temperature. This transition takes place for a critical value Δ_c of the vibron-phonon coupling. From our numerical data, it appears that the behavior of Δ_c is well reproduced by the following law:

$$\Delta_c = 2.11 \frac{\hat{\Phi}^2}{\hat{A}} \left(\frac{\Omega_0}{kT} \right)^{0.48}. \tag{36}$$

Although Eq. (36) does not have any physical signification, it clearly shows that Δ_c decreases with both the temperature and the intramolecular anharmonicity. The temperature dependence indicates that the confinement of the vibron pair is due to effective potential barriers which the high depends on the temperature. Indeed, the thermal fluctuations of the number of dilated phonons produces an effective frequency shift for each defect which the amplitude increases with the temperature. By contrast, the influence of the intramolecular anharmonicity characterizes the breatherlike behavior of the TVBS. As when the anharmonicity is increased, their capacity to delocalize decreases so that the influence of the disorder is enhanced.

APPENDIX A: PHONON DILATATION AND DRESSED VIBRON

To understand the dressing effect produced by the local dilatation of the phonon field, let us consider the single vibron fundamental eigenstate of the local Hamiltonian H_n [Eq. (4)]. This state, expressed in terms of the unitary transformation Eq. (5) as $|\Psi(1_n,0_n)\rangle = U_n^+[\theta(1)]|1_n,0_n\rangle$, appears as a linear superimposition of unperturbed phonon states as

$$|\Psi(1_n,0_n)\rangle = \sum_{p_n} \xi_{p_n} |1_n,p_n\rangle, \tag{A1}$$

where $\xi_{p_n} = \langle p_n | U_n[-\theta(1)] | 0_n \rangle$ denotes the weight of the state involving p_n unperturbed phonons. After some algebraic calculations, it is straightforward to show that this weight is written as

$$\xi_p = \frac{1}{(p/2)!} \sqrt{\frac{p!}{\cosh[\theta(1)]}} \left(\frac{-\tanh[\theta(1)]}{2} \right)^{p/2} \tag{A2}$$

for even p values whereas $\xi_p = 0$ for odd p values. Therefore, by introducing Eq. (A2) into Eq. (A1), the single vibron state is finally expressed as

$$|\Psi(1_n,0_n)\rangle = \frac{\exp\left(-\frac{\tanh[\theta(1)]}{2} a_n^{+2} \right)}{\sqrt{\cosh[\theta(1)]}} |1_n,0_n\rangle. \tag{A3}$$

APPENDIX B: AVERAGE DRESSING OPERATOR

By assuming the optical phonons in thermal equilibrium at the temperature T, the average value of the nth dressing operator is expressed in terms of the dilatation operator U_n as

$$\langle \Theta_n^{\pm} \rangle = \sum_{p_n=0}^{\infty} \langle p_n | U_n(\alpha_n^{\pm}) | p_n \rangle (1 - e^{-\beta\Omega_0}) e^{-p_n \beta \Omega_0}, \tag{B1}$$

where $\alpha_n^{\pm} = \theta(N_n) - \theta(N_n \mp 1)$. Within the coordinate representation, Eq. (B1) can be rewritten in terms of the wave functions $\varphi_{p_n}(x)$ connected to the nth harmonic mode and defined as

$$\varphi_{p_n}(x) = \frac{e^{-x^2/2}}{\sqrt{\pi^{1/2} 2^{p_n} p_n!}} H_{p_n}(x), \tag{B2}$$

where $H_{p_n}(x)$ denotes the p_nth Hermite polynomial. Therefore, by taking into account on the scaling introduced by the dilatation operator, i.e., $U_n(\alpha)\varphi_{p_n}(x) \to e^{-\alpha/2}\varphi_{p_n}(e^{-\alpha}x)$, Eq. (B1) is rewritten as

$$\langle \Theta_n^{\pm} \rangle = (1 - e^{-\beta\Omega_0}) e^{-\alpha_n^{\pm}/2} \int \frac{dx}{\sqrt{\pi}} e^{-(1+e^{-2\alpha_n^{\pm}})x^2/2} \times \sum_{p_n=0}^{\infty} \frac{H_{p_n}(x) H_{p_n}(e^{-\alpha_n^{\pm}} x)}{p_n!} \left(\frac{e^{-p_n \beta \Omega_0}}{2} \right)^{p_n}. \tag{B3}$$

Therefore, by using the Mehler's Hermite polynomial formula

$$\sum_{n=0}^{\infty} \frac{H_n(x) H_n(y)}{n!} \left(\frac{w}{2} \right)^n = (1 - w^2)^{-1/2} \times \exp\left(\frac{2xyw - (x^2 + y^2)w^2}{1 - w^2} \right), \tag{B4}$$

it is straightforward to show that the average value of the dressing operator is finally written as

$$\langle \Theta_n^{\pm} \rangle = \frac{1}{\sqrt{\cosh^2(\alpha_n^{\pm}/2) + \coth^2(\beta\Omega_0/2) \sinh^2(\alpha_n^{\pm}/2)}}. \tag{B5}$$

*Electronic address: vincent.pouthier@univ-comte.fr

[1] V. Pouthier, C. Girardet, and J. C. Light, J. Chem. Phys. **114**, 4955 (2001).
[2] V. Pouthier and C. Girardet, Phys. Rev. B **65**, 035414 (2002).
[3] V. Pouthier, J. Chem. Phys. **118**, 3736 (2003).
[4] V. Pouthier, J. Chem. Phys. **118**, 9364 (2003).
[5] V. Pouthier, Phys. Rev. B **71**, 115401 (2005).
[6] V. Pouthier, Physica D **213**, 1 (2006).
[7] C. Falvo and V. Pouthier, J. Chem. Phys. **122**, 014701 (2005).
[8] A. S. Davydov and N. I. Kisluka, Phys. Status Solidi B **59**, 465 (1973); Zh. Eksp. Teor. Fiz. **71**, 1090 (1976) [Sov. Phys. JETP **44**, 571 (1976)].
[9] S. Aubry, Physica D **103**, 201 (1997).
[10] S. Flach and C. R. Willis, Phys. Rep. **295**, 181 (1998).
[11] R. S. MacKay, Physica A **288**, 174 (2000).
[12] P. Guyot-Sionnest, Phys. Rev. Lett. **67**, 2323 (1991).
[13] R. Honke, P. Jakob, Y. J. Chabal, A. Dvorak, S. Tausendpfund, W. Stigler, P. Pavone, A. P. Mayer, and U. Schröder, Phys. Rev. B **59**, 10996 (1999).
[14] R. P. Chin, X. Blase, Y. R. Shen, and S. GT. Louie, Europhys. Lett. **30**, 399 (1995).
[15] D. J. Dai and G. E. Ewing, Surf. Sci. **312**, 239 (1994).
[16] P. Jakob, Phys. Rev. Lett. **77**, 4229 (1996).
[17] P. Jakob, Physica D **119**, 109 (1998).
[18] P. Jakob, J. Chem. Phys. **114**, 3692 (2001).
[19] P. Jakob, Appl. Phys. A: Mater. Sci. Process. **75**, 45 (2002).
[20] P. Jakob and B. N. J. Persson, J. Chem. Phys. **109**, 8641 (1998).
[21] H. Okuyama, T. Ueda, T. Aruga, and M. Nishijima, Phys. Rev. B **63**, 233404 (2001).
[22] V. Fleuro, Chaos **13**, 676 (2003).
[23] J. C. Eilbeck, in *Proceedings of the Third Conference Localization and Energy Transfert in Nonlinear Systems*, edited by L. Vasquez, R. S. Mackay, and M. P. Zorzano (World Scientific, Singapore, 2003).
[24] J. C. Kimball, C. Y. Fong, and Y. R. Shen, Phys. Rev. B **23**, 4946 (1981).
[25] F. Bogani, G. Cardini, V. Schettino, and P. L. Tasselli, Phys. Rev. B **42**, 2307 (1990).
[26] A. C. Scott, J. C. Eilbeck, and H. Gilhoj, Physica D **78**, 194 (1994).
[27] L. Proville, Phys. Rev. B **71**, 104306 (2005).
[28] H. Frochlich, Adv. Phys. **3**, 325 (1954).
[29] D. W. Brown and Z. Ivic, Phys. Rev. B **40**, 9876 (1989).
[30] D. W. Brown, K. Lindenberg, and X. Wang, in *Davydov's Soliton Revisited*, edited by P. L. Christiansen and A. C. Scott (Plenum, New York, 1990).
[31] Z. Ivic, D. Kapor, M. Skrinjar, and Z. Popovic, Phys. Rev. B **48**, 3721 (1993).
[32] Z. Ivic, D. Kostic, Z. Przulj, and D. Kapor, J. Phys.: Condens. Matter **9**, 413 (1997).
[33] J. Tekic, Z. Ivic, S. Zekovic, and Z. Przulj, Phys. Rev. E **60**, 821 (1999).
[34] Z. Ivic, Z. Przulj, and D. Kostic, Phys. Rev. E **61**, 6963 (2000).
[35] V. Pouthier, Phys. Rev. E **68**, 021909 (2003).
[36] V. Pouthier and C. Falvo, Phys. Rev. E **69**, 041906 (2004).
[37] V. Pouthier, Phys. Rev. E **72**, 031901 (2005).
[38] B. N. J. Persson and R. Ryberg, Phys. Rev. B **32**, 3586 (1985).
[39] B. N. J. Persson and R. Ryberg, Phys. Rev. Lett. **54**, 2119 (1985).
[40] B. N. J. Persson, F. M. Hoffmann, and R. Ryberg, Phys. Rev. B **34**, 2266 (1986).
[41] F. M. Hoffmann and B. N. J. Persson, Phys. Rev. B **34**, 4354 (1986).
[42] B. N. J. Persson and F. M. Hoffmann, J. Chem. Phys. **88**, 3349 (1988).
[43] P. Jakob and B. N. J. Persson, Phys. Rev. B **56**, 10644 (1997).
[44] P. Jakob and B. N. J. Persson, Phys. Rev. Lett. **78**, 3503 (1997).
[45] B. N. J. Persson, Phys. Rev. B **46**, 12701 (1992).
[46] R. Zwanzig, Lect. Theor. Phys. **3**, 106 (1960).
[47] B. Kramer and A. MacKinnon, Rep. Prog. Phys. **56**, 1469 (1993).
[48] D. J. Thouless, Phys. Rep., Phys. Lett. **13**, 93 (1974).
[49] J. T. Edwards and D. J. Thouless, J. Phys. C **5**, 807 (1972).
[50] V. L. Berezinski and L. P. Gorkov, Zh. Eksp. Teor. Fiz. **78**, 812 (1980) [Sov. Phys. JETP **51**, 409 (1980)].
[51] A. D. Mirlin, Phys. Rep. **326**, 259 (1998).